LOSS ESTIMATION OF FINITE LENGTH MICROSTRIP LINE

P. Supannkoon P. Rawiwan M. Chamchoy P. Tangtisanon
S. Promwong† and J. Takada†

Department of Industrial Technology, Faculty of Engineering, King Mongkut's Institute of Technology Ladkrabang Chalongkrung Rd., Ladkrabang, Bangkok 10520, Thailand
E-mail: kpsathap@kmitl.ac.th
†INCOCSAT, Tokyo Institute of Technology, Japan

I. Introduction

It is well known that both conductor loss and dielectric loss are essential loss factors in lossy microstrip line. On the other hand, lossless transmission line does not suffer from these losses at any length and frequency. When the line length is finite, however, some transmission losses are observed even for the lossless microstrip line. It means that a part of the input power is transformed into other modes, which may cause cross talk unexpected radiation, resonance etc, in PCB. This paper discusses about the mechanism of how these losses are generated in the finite microstrip line. The surface wave loss and the radiation loss are evaluated by using FDTD via the Poynting vector.

In section II of this paper, a brief review of FDTD method adapted for lossless microstrip line analysis is presented together with the models matched to the microstrip line of the voltage source and the load. The computation of the Poynting vector is also discussed in this section.

In section III, the method is used for the analysis of lossless microstrip line structure with finite length to evaluate the losses due to radiation wave and surface wave.

II. Formulation of the problem

A. Finite-Difference Equation

The finite-difference equations are derived directly from Maxwell's curl equations in the time-domain. For the lossless microstrip line,the strip and the ground plane are made of a perfect conductor ($\sigma = \infty$) which has zero thickness, and the substrate has a relative dielectric constant of ϵ_r. To obtain discrete approximation to the continuous partial differential equation, the centered difference approximation is used on both the time and space first-order partial derivatives. After simple arrangement, the finite difference equations are described [1]. For the electric field components on the interface of the two different dielectric materials, the average of dielectric constant $(\epsilon_1 + \epsilon_2)/2$ is used as permittivity. The maximum time step is limited by the stability restriction of finite difference equation.

B. Voltage Source and Resistor Model

A voltage source is represented as an electric field E in the z direction at the node i_s, j_s and k_s along x, y and z axes, respectively. If the source resistance is set to R_s then the usual FDTD electric field at the source location is given by [2]

$$E_z\Big|^n_{i_s,j_s,k_s} = \frac{1}{\Delta z} V_s\Big|^n + \frac{R_s}{\Delta z} I_s\Big|^{n-1/2}, \tag{1}$$

when the current though the source is given by

$$I_s\Big|^{n-1/2} = \frac{H_y\Big|^{n-1/2}_{i+1/2,j,k} - H_y\Big|^{n-1/2}_{i-1/2,j,k}}{\Delta x} - \frac{H_x\Big|^{n-1/2}_{i,j+1/2,k} - H_x\Big|^{n-1/2}_{i,j-1/2,k}}{\Delta y}. \tag{2}$$

For the resistor, voltage source V_s is simply set to be zero.

C. Excitation Pulse

A wideband Gaussian pulse with finite DC constant is desirable as the excitation because its frequency spectrum is also Gaussian. Therefore, it will provide frequency-domain information from DC to the desired cutoff frequency by adjusting the width of the pulse. The wideband Gaussian pulse will have the following expression,

$$V_s\,|^n = V_0 e^{-\left(\frac{n-n_0}{n_{decay}}\right)^2}, \tag{3}$$

where n is the time step. The pulse has maximum amplitude V_0 at time step n_0 and has a $1/e$ characteristic decay of n_{decay} time step.

D. Absorbing Boundary Condition Treatment

One of the six mesh boundaries is a ground plane and its tangential field values are forced to be zero. The tangential field components on the other five mesh walls must be specified in such a way that outgoing waves are not reflected. The perfectly matched layer absorbing boundary condition (PML ABC) [3] is used in this paper.

E. Poynting Vector and Total Power

To determine Poynting vector by using FDTD method, the average field components at the center of unit cell must be obtained. Then, the average filed components at center of node i, j and k can be written as

$$\overline{E_x}\,\Big|^n_{i,j,k} = \frac{E_x\,\Big|^n_{i-1j,k} + E_x\,\Big|^n_{i,j,k}}{2}, \tag{4}$$

$$\overline{E_y}\,\Big|^n_{i,j,k} = \frac{E_y\,\Big|^n_{i,j-1,k} + E_y\,\Big|^n_{i,j,k}}{2}, \tag{5}$$

$$\overline{E_z}\,\Big|^n_{i,j,k} = \frac{E_z\,\Big|^n_{i,j,k-1} + E_z\,\Big|^n_{i,j,k}}{2}, \tag{6}$$

$$\overline{H_x}\,\Big|^n_{i,j,k} = \frac{H_x\,\Big|^n_{i,j-1,k-1} + H_x\,\Big|^n_{i,j,-1,k} + H_x\,\Big|^n_{i,j,k-1} + H_x\,\Big|^n_{i,j,k}}{4}, \tag{7}$$

$$\overline{H_y}\,\Big|^n_{i,j,k} = \frac{H_y\,\Big|^n_{i-1,j,k-1} + H_y\,\Big|^n_{i-1,j,k} + H_y\,\Big|^n_{i,j,k-1} + H_x\,\Big|^n_{i,j,k}}{4}, \tag{8}$$

$$\overline{H_z}\,\Big|^n_{i,j,k} = \frac{H_z\,\Big|^n_{i-1,j-1,k} + H_z\,\Big|^n_{i-1,j,k} + H_z\,\Big|^n_{i,j-1,k} + H_x\,\Big|^n_{i,j,k}}{4}, \tag{9}$$

The vector of each component in frequency domain can be determined by using Fourier transformation of the average fields in time domain. These vectors may by written as

$$\mathcal{E}_{i,j,k} = \mathcal{F}\left\{\overline{E_x}\,\Big|^n_{i,j,k}\right\}\overline{a_x} + \mathcal{F}\left\{\overline{E_y}\,\Big|^n_{i,j,k}\right\}\overline{a_y} + \mathcal{F}\left\{\overline{E_z}\,\Big|^n_{i,j,k}\right\}\overline{a_z}, \tag{10}$$

$$\mathcal{H}_{i,j,k} = \mathcal{F}\left\{\overline{H_x}\,\Big|^n_{i,j,k}\right\}\overline{a_x} + \mathcal{F}\left\{\overline{H_y}\,\Big|^n_{i,j,k}\right\}\overline{a_y} + \mathcal{F}\left\{\overline{H_z}\,\Big|^n_{i,j,k}\right\}\overline{a_z}, \tag{11}$$

where Poynting at node i, j and k defined as

$$\mathcal{W}\,|_{i,j,k} = \mathcal{E}\,|_{i,j,k} \times \mathcal{H}\,|_{i,j,k}\,. \tag{12}$$

The total power crossing a surface can be obtained by

$$P = \int\int_s \mathcal{W}\cdot\hat{n}\,da, \tag{13}$$

where $\hat{n}$ is unit vector normal to the surface.

III. Numerical Results

Radiation and surface wave losses of finite length microstrip line are estimated by FDTD simulation. The dimension of the microstrip line analyzed is shown in Figure 1. The parameters of the structure are as follows:

Width of substrate: $W_s = 13.8$ mm. Width of metal strip: $W = 1.8$ mm.

Thickness of substrate: $h = 0.6$ mm. Length of metal strip: $l = 5.0$ mm.

Thickness of metal strip: $t = 0$ mm. Permittivity of substrate: $\epsilon_r = 2.29$

To accommodate the structural details of the microstrip line, the FDTD parameters are chosen as Mesh parameters:

$\Delta x = 0.3$ mm. $\Delta y = 0.5$ mm. $\Delta z = 0.2$ mm. $\Delta t = 0.52668$ ps.

The voltage source V_s and the resistor R_s are connected in between microstrip line at one end and the load resistance R_L is connected at the other end as in Figure 1 and explained in II.B. Source and load impedances are $R_s = R_L = 50\Omega$, which are matched to the characteristic impedance of the microstrip line at a low frequency. To study about the much the losses are generated in lossless microstrip line, the transmission efficiency η should be defined as

$$\eta(f) = \frac{P_L(f)}{P_{L,max}(f)}, \tag{14}$$

where $P_{L,max}(f)$ is the maximum available power of the load at frequency f and is defined as

$$P_{L,max}(f) = \frac{V_s^2(f)}{8R_L}. \tag{15}$$

where $V_s(f)$ is the frequency component of source voltage η is determined by the radiation and surface wave losses as well as by the mismatch losses.

The computed transmission efficiency by using FDTD method is shown in Figure 2. From significant losses are observed at the higher frequency. The two dominant loss factors are the radiation and the surface wave. The losses due to the radiation and surface wave defined as those powers normalized by the maximum available power at the load. Figures 3 (a) and (b) show the boundaries of integration to estimate the power of surface wave and radiation, respectively. The shaded regions in Fig. 3 (a) represent the radiation wave which occurred at the topside of the microstrip line and in Fig. 3 (b) represent the radiation wave which occurred on the front-back side of the microstrip line.

Figure 4 shows the radiation power and surface wave of the lossless microstrip line with a finite length. It can be observed that the radiation power is about 5 dB higher than surface wave and it decreases when the frequency is above 15 GHz. The peak corresponds to the resonance at $\lambda/2$ of the strip. Figure 5 shows a comparison between radiation power at the front-back side of the microstrip line and its topside. The radiated power at the both sides is about 17 dB higher than at the topside in average.

IV. Conclusion

In this paper, the mechanism of the loss generation in the lossless microstrip line with finite length is quantitatively studied. These losses are caused due to the radiation wave and the surface wave. Therefore, the power of both waves is analyzed by using FDTD via Poynting vector integration. From numerical result, it is found that majority of loss is the radiation from the topside of microstrip line.

References

[1] Yee, K. S., "Numerical solution of initial boundary value problems involving Maxwell's equations in isotropic media," IEEE Trans. Antennas and propagation, vol. 14, pp. 302-307, 1996.

[2] R. J. Luebbers and H.S.Langdon, "A simple feed model reduces time steps needed for FDTD antenna and microstrip calculations," IEEE Trans. Antennas and Propagation, vol. 44, no. 7, pp. 1000-1005, Jul. 1996.
[3] Berenger, J. -P., "A perfectly matched layer for the absorption of electromagnetic waves," J. Computational Physics, vol. 114, pp. 185-200, 1994.

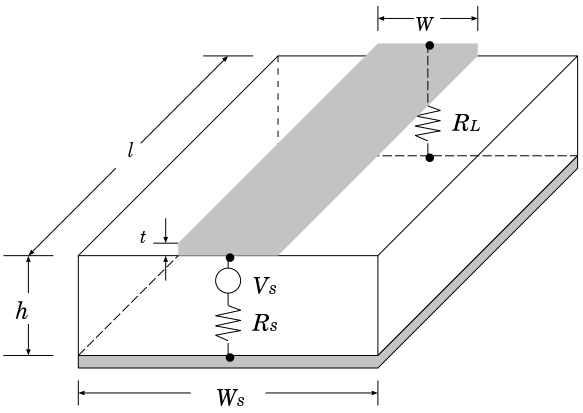

Fig. 1. Microstrip line structure.

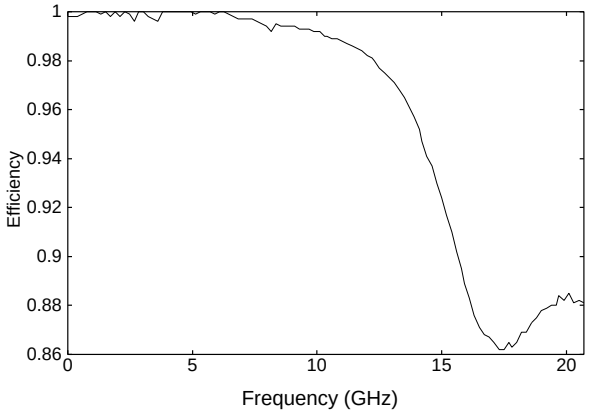

Fig. 2. Computed transmission efficiency.

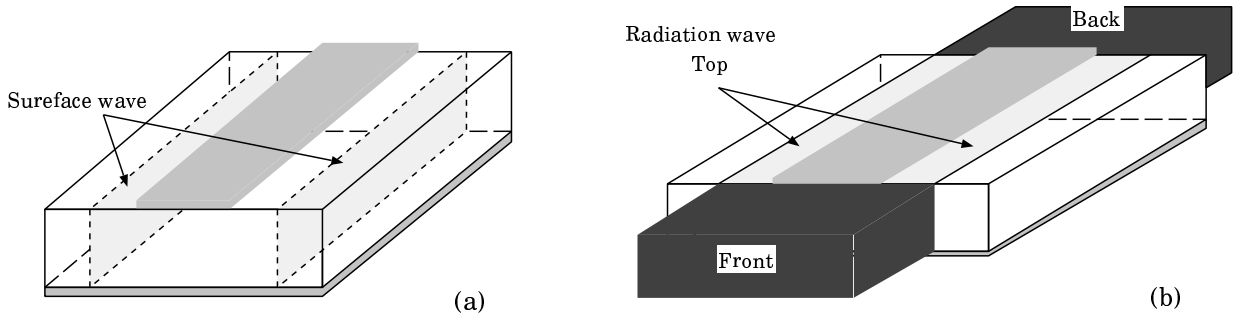

Fig. 3. Boundary condition for evaluating power of radiation wave and surface wave.

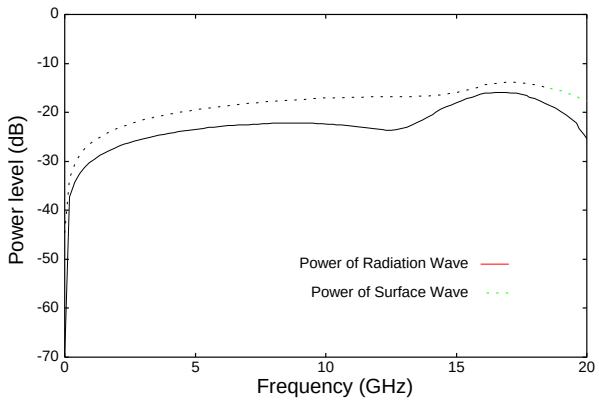

Fig. 4. Computed power of radiation wave and surface wave.

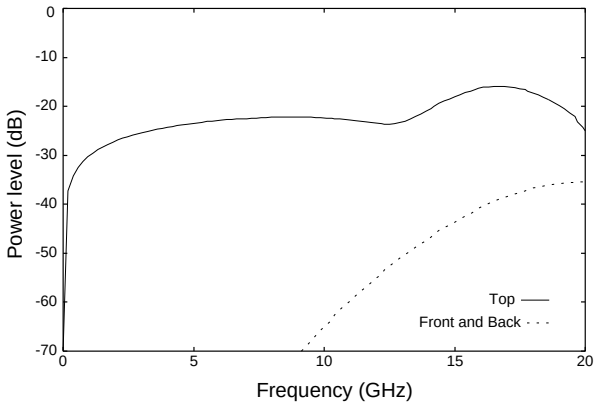

Fig. 5. Power of radiation wave at top side compared with that at front and back side of microstrip line.